



Synthesis and Mesomorphic Behavior of Two New Homologous Series Containing Azobenzene and 1,3,4-Oxadiazole Units

Nisreen H. Karam, Amir T. Atto & Ammar H. Al-dujaili

To cite this article: Nisreen H. Karam, Amir T. Atto & Ammar H. Al-dujaili (2014) Synthesis and Mesomorphic Behavior of Two New Homologous Series Containing Azobenzene and 1,3,4-Oxadiazole Units, *Molecular Crystals and Liquid Crystals*, 605:1, 1-11, DOI: [10.1080/15421406.2013.840944](https://doi.org/10.1080/15421406.2013.840944)

To link to this article: <http://dx.doi.org/10.1080/15421406.2013.840944>



Published online: 15 Dec 2014.



Submit your article to this journal [↗](#)



Article views: 66



View related articles [↗](#)



View Crossmark data [↗](#)

Synthesis and Mesomorphic Behavior of Two New Homologous Series Containing Azobenzene and 1,3,4-Oxadiazole Units

NISREEN H. KARAM, AMIR T. ATTO,
AND AMMAR H. AL-DUJAILI*

Department of Chemistry, College of Education of Pure Science,
Ibn Al-Haytham, University of Baghdad, Baghdad, Iraq

Two new nonsymmetrical mesogenic homologous series of terminal substituent ether (series [V_n]) and carboxy (series [VI_n]) incorporating azobenzene and 1,3,4-oxadiazole group were synthesized. Both series have been All compounds thus isolated were purified and characterized by elemental analysis, Fourier Transform Infrared Spectroscopy, ¹H NMR, along with thermal analysis and texture observation using Differential Scanning Calorimetry (DSC) and Polarizing Optical Microscopy (POM), respectively. All compounds of the first series exhibited liquid crystalline properties. The homologues [V₁]-[V₃] display a nematic mesophase, the compounds [V₄]-[V₇] exhibit a dimorphism behavior, nematic (N) and smectic A (SmA) mesophases, the compounds [V₈] and [V₉] display enantiotropic smectic A and C (SmA and SmC) phases and the last homologue [V₁₂] exhibits only a smectic C mesophase. All compounds of the second series [VI_n] also show mesomorphic behavior, the compounds [VI₁]-[VI₃] and [VI₅] display the nematic mesophase, the homologue [VI₇] exhibits dimorphism behavior, nematic, and smectic A (SmA). The mesomorphic behavior has been analyzed in terms of structural property relationships.

Keywords Azobenzene; liquid crystals; nonsymmetrical-1,3,4-oxadiazole

Introduction

Many series of liquid crystalline compounds containing heterocyclic units have been synthesized due to their potentially wide range of applications, such as in the optical, electrical, and biological medical fields [1–4]. Interest in these compounds arises because the inclusion of heteroatom can cause large changes in the kind of mesophase present or in the physical properties of the phases.

Many series of liquid crystalline compounds containing heterocyclic groups have been synthesized due to their potentially wide range of applications, such as in the optical, electrical, and biological medical fields [5–7]. Usually five member heterocycles are involved and they form part of the core in rod-shaped, bent-shaped, or disc-shaped molecules.

*Address correspondence to Ammar H. Al-Dujaili, Department of Chemistry, College of Education for Pure Science, Ibn Al-Haytham, University of Baghdad, Baghdad, Iraq; E-mail: ammar.h.s.@ihcoedu.uobaghdad.edu.iq; ah.aldujaili1946@gmail.com

Color versions of one or more of the figures in the article can be found online at www.tandfonline.com/gmcl.

Among the heterocyclic mesogenes, much attention has been paid to 2,5-disubstituted 1,3,4-oxadiazoles owing to their rich mesophases and good thermal stability. In addition, this type of liquid crystal emits strong fluorescent light with high quantum yield and many potentially be used as functional materials [8–10].

Cionaca et al. [11] have described the liquid-crystalline properties of some 2,5-asymmetric disubstituted 1,3,4-oxadiazole derivatives containing an azo and an ester linkage obtained through esterification of 2-(4-methoxyphenyl)-5-(4-hydroxyphenyl)-1,3,4-oxadiazole with a series of 4-(4-alkoxyphenyl)-benzoic acids containing 6–10 and 18 aliphatic carbon atoms. All reported compounds present liquid crystalline properties, with nematic and smectic C type structures, with very large range of stability of mesophases.

Bai et al. [12] have reported the synthesis and mesomorphic behavior of a series of nonsymmetric liquid crystal dimers with long terminal chains containing 1,3,4-oxadiazole group and azobenzene group as the mesogenic units. These nonsymmetric liquid crystal dimers are evidenced to display monolayer smectic A phase. Microphase segregation and specific intermolecular interactions between the two different mesogenic units are the major driving forces for the formation of the monolayer smectic A structure.

Continuing our work on the LC possibilities of oxadiazole and thiadiazole systems [13,14], we describe in this paper the synthesis and liquid crystalline properties of two new homologous series containing azobenzene and 1,3,4-oxadiazole group.

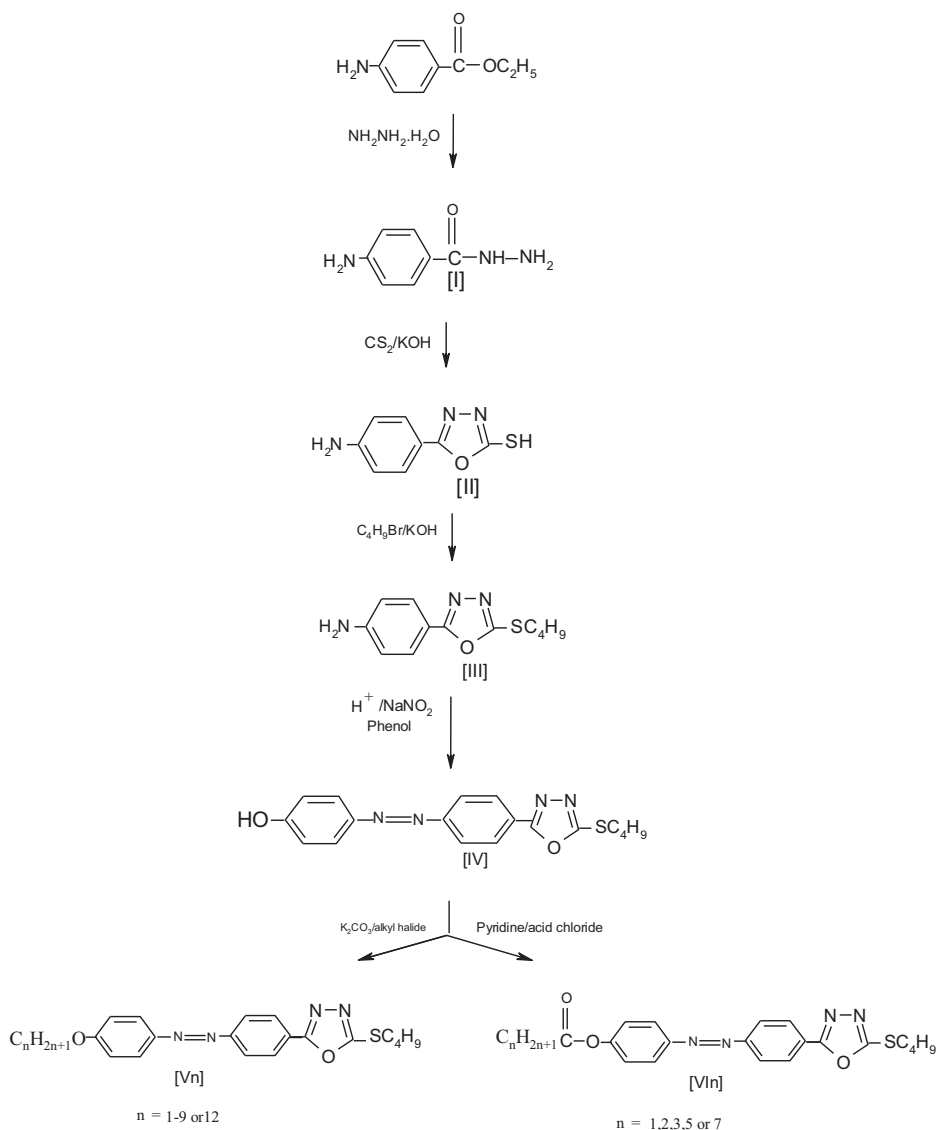
Experimental

Materials

All chemicals and solvents were of reagent grade (Aldrich Chemicals Co.) and used without further purification.

Instrumentation

Elemental analyses (CHN) were carried out using a Perkin-Elmer model 2400 instrument. Infrared spectra were recorded with a Shimadzu 8000 FT-IR spectrophotometer in the wave number range $4000\text{--}400\text{ cm}^{-1}$ with samples embedded in KBr disc. ^1H NMR spectra were obtained with Bruker spectrometer model ultra shield at 300 MHz. The compounds were dissolved in $\text{DMSO-}d_6$ solution with the TMS as internal standard. Mass spectra were recorded on IEOL JMS-7 high resolution instrument. Transition temperatures and enthalpies were scanned in TA instruments Q1000 DSC, differential scanning calorimeter with a heating rate of 10.0°C/min in air and it was calibrated with indium (156.6°C , 28.45 J/g). The temperatures were read as the maximum of the endothermic peaks. The textures of the mesophases were studied with Olympus BX40 microscope equipped with a Leitz Laborlux 12 Pol's hot stage and PR600 controller. The samples were investigated using cross polarizers at room temperature with a magnification of $2.5\times$ and a magnification $10\times$ or $20\times$ was at elevated temperature. The samples were mounted on quartz slides of 26.26 mm with 1 mm thickness. Procedure: The substance to be examined is heated up to the isotropic liquid point on a microscopic slide and a cover slip is pushed into the melt in such a way that thin layer is formed between the slide and cover slip. The slide was cooled thoroughly and placed on the heating stage of the polarizing microscope. The temperature initially was raised rapidly (5°C/min) and the slide was then recooled. Afterward, the heating was then continued at a rate of 1°C/min and cooling too was carried out at the same rate. The mesomorphic transition temperatures and the textures under the microscope were recorded for the compounds.



Scheme 1.

Synthesis

The reaction sequences leading to the formation of compounds of the two series 2-butylthio-5-[4-(4'-alkoxyphenyl) azophenyl]-1,3,4-oxadiazol [**V_n**] and 2-butylthio-5-[4-(4'-carboxyalkylphenyl) azophenyl]-1,3,4-oxadiazol [**VI_n**] are outlined in Scheme 1, where *n* designate the number of carbon atom in terminal alkoxy or carboxyalkyl group substituent.

Synthesis of 4-aminophenyl hydrazide [I]. This compound was synthesized by the method described in references [15,16].

Synthesis of 2-thio-5-[4-aminophenyl]-1,3,4-oxadiazole [III]. This compound was synthesized by the method described in references [17,18].

Synthesis of 2-butylthio-5-(4-aminophenyl)-1,3,4-oxadiazole [IIII]. Potassium hydroxide (0.67 g, 12 mmol) dissolved in minimum amount of water, was added dropwise to a stirred solution of (II) (1.93 g, 10 mmol) in 10 mL of dioxane at 5°C. After heating the mixture for 15 min and cooling, *n*-butyl bromide (1.37 g, 10 mmol) was added dropwise. The solution was refluxed for 2 hr; afterward the solvent was evaporated on a rotatory evaporator. Ice water (100 mL) was added; the resulting precipitate was collected, and recrystallized from ethanol, yield (78%). M.P. 115°C. Calc. for C₁₂H₁₅ON₃S; C, 57.83; H, 6.02; N, 16.87; Found: C, 57.03; H, 5.94; N, 16.76. FT-IR (KBr, cm⁻¹): 3350–3440 (ν_{NH₂}, amine); 2990–2950 (ν_{C-H}, aliphatic); 1620 (ν_{C=N}, oxadiazole ring). ¹H NMR (DMSO): δ = 6.5–7.8 ppm (d-d, C₆H₄); 6.0–6.5 (b, NH₂); 3.1–3.5 (t, S-CH₂); 1.3–1.9 (m, CH₂CH₂); 0.9–1.2 (t, CH₃). MS: m/z+1 = 250.

Synthesis of 2-butylthio 5-[4-(4'-hydroxyphenyl) azophenyl]-1,3,4-oxadiazole [IV]. A mixture of (6.23 g, 25 mmol) of [IIII] and 15 mL of concentrated H₃PO₄ was gently heated and stirred until all was dissolved; it was then cooled to 0°C and 5 mL of concentrated HNO₃ was added. Sodium nitrite (1.76 g, 25 mmol) dissolved in a very small amount of water was added portion-wise. During this addition the temperature was kept between –5°C and 0°C. After vigorously stirring for 10 min, (2.54 g, 27 mmol) of phenol were added quickly; stirring and the low temperature were maintained for 3 hr. The reaction mixture was then poured over ice, giving the crude product which was then filtered and recrystallized from ethanol, yield (90%). M.P. 170–173°C. Calc. for C₁₈H₁₈O₂N₄S; C, 61.01; H, 5.08; N, 15.82; Found: C, 60.66; H, 5.94; N, 15.25. FT-IR (KBr, cm⁻¹): 3180 (ν_{OH}, hydroxy); 3010–2990 (ν_{C-H}, aliphatic); 1660 (ν_{C=N}, oxadiazole ring). ¹H NMR (DMSO): δ = 6.5–7.8 ppm (d-d, C₆H₄); 6.0–6.5 (b, NH₂); 3.1–3.5 (t, S-CH₂); 1.3–1.9 (m, CH₂CH₂); 0.9–1.2 (t, CH₃). MS: m/z+1 = 393. MS: m/z+1 = 355.

Synthesis of 2-butylthio-5-[4-(4'-alkoxyphenyl) azophenyl]-1,3,4-oxadiazol [V_n]. A mixture of [IV] (3.54 g, 10 mmol), anhydrous potassium carbonate (5.53 g, 40 mmol), cyclohexane 35 mL and *n*-alkyl bromide or alkyl iodide (18 mmol) were refluxed and stirred vigorously. Alkylation was completed after 3 hr. The solution filtered from potassium carbonate, the solvent was distilled off, and the product was extracted by adding 25 mL of 10% aqueous KOH and 50 mL of ethyl acetate. The organic layer was dried over anhydrous MgSO₄; ethyl acetate was evaporated to give the compounds [V_n].

n	1	2	3	4	5	6	7	8	9	12
Yields (%)	85	92	98	96	94	96	95	92	90	80

Data Compound [V₁]

Yield (85%). M.P. 112°C. Calc. for C₁₉H₂₀O₂N₄S; C, 61.96; H, 5.43; N, 15.22; Found: C, 62.12; H, 4.64; N, 15.80. FT-IR (KBr, cm⁻¹): 2995–2850 (ν_{C-H}, aliphatic); 1620 (ν_{C=N}, oxadiazole ring); 1070 (ν_{C-O-C}, OCH₃). ¹H NMR (DMSO): δ = 7.1–8.1 ppm (d-d, C₆H₄); 3.83 (s, OCH₃); 3.39 (t, S-CH₂); 1.2–1.9 (m, CH₂CH₂); 0.95 (t, CH₃). MS: m/z+1 = 369.

Synthesis of 2-butylthio-5-[4-(4'-carboxyalkylphenyl) azophenyl]-1,3,4-oxadiazol [VI_n].

To a stirred solution of compound [IV] (3.54 g, 10 mmol), triethylamine (2.02 g, 20 mmol) in dried mixture of (5 mL DMF + 10 mL THF), was added dropwise carboxylic acid chloride (10 mmol) at 0–5°C. After addition has been completed the resulting suspension was stirred at the same temperature for 3 hr. The triethylamine hydrochloride salt was precipitated. It was filtered and filtrate was poured with stirring into 100 mL ice water, then the mixture was extracted by adding 50 mL of diethyl ether. The ether solution was evaporated to give a residue which was recrystallized from ethanol/water, yield 72–88%.

n	1	2	3	5	7
Yields (%)	83	72	86	88	80

Data Compound [VI₁]

Yield (83%). M.P. 119°C. Calc. for C₂₀H₂₀O₃N₄S; C, 60.61; H, 5.05; N, 14.14; Found: C, 61.51; H, 5.00; N, 13.77. FT-IR (KBr, cm⁻¹): 2950–2850 (ν_{C-H}, aliphatic); 1757 (ν_{C=O}, carboxy); 1070 (ν_{C-O-C}, OCH₃). ¹HNMR (DMSO): δ = 7.1–8.1 ppm (d-d, C₆H₄); 3.53 (s, C(O)CH₃); 3.39 (t, S-CH₂); 1.88 (m, CH₂CH₂); 0.93 (t, CH₃). MS: m/z+1 = 397.

Result and Discussion*Characterization of Compounds*

The synthetic routes used for the preparation of the 15 compounds of the two series [V_n] and [VI_n] are outlined in Scheme 1. The elemental analysis of series [V_n] and [VI_n] compounds synthesized above is listed in Table 1. The observed values are in well agreement with theoretical values indicating structure of respective compounds. The structures of final products were confirmed by ¹HNMR and FT-IR spectroscopy. In ¹HNMR spectra, the synthesized [V_n] compounds showed peaks of the terminal oxy ether spacer (-OCH₂(CH₂)_nCH₃) at ≈4.37–3.59 ppm and for the [VI_n] compounds the peaks of the terminal thio ether spacer (-S(CH₂)_nCH₃) at ≈3.38–1.11 ppm. The IR spectral frequencies of the synthesized [V_n] and [VI_n] compounds were obtained using KBr pellets. For [V_n] compounds the absorption peaks of C-O-C and C = N were observed at 1070 and 1620 cm⁻¹, respectively, along with aliphatic C-H stretching frequencies at 2995–2850 cm⁻¹. For [VI_n] compounds The absorption peak of carboxy group was observed at 1757 cm⁻¹ and C-O-C stretching frequencies occurred at 1070 cm⁻¹ along with aliphatic C-H stretching frequencies at 2950–2850 cm⁻¹.

Liquid-Crystalline Properties

The mesomorphic properties for these two ([V_n] and [VI_n]) series were determined by means of DSC and POM. DSC is a valuable aid by which phase transition temperature can be conveniently measured. This techniques offers a direct and complimentary (to microscopy) evaluation of thermal behavior.

The thermal and thermodynamic data for the compounds of [V_n] and [VI_n] series are gathered in the formalTables 2 and 3, respectively. A plot of transition temperature against the number (n) of carbon atoms in the lateral alkoxy chain is shown in Figs. 1 and 2. The effects of the terminal chain length on the transition temperatures and phases behavior observed in this series are in accordance with those observed for conventional

Table 1. Elemental analysis data for the series $[V_n]$ and $[VI_n]$

Compound	Molecular formula	Molecular weight (g/mol)	Analysis% found (calcd.)		
			C	H	N
$[V_1]$	$C_{19}H_{20}O_2N_4S$	368	62.12 (61.95)	4.64 (5.43)	15.80 (15.21)
$[V_2]$	$C_{20}H_{22}O_2N_4S$	382	63.20 (62.82)	5.89 (5.75)	14.51 (14.65)
$[V_3]$	$C_{21}H_{24}O_2N_4S$	396	64.23 (63.63)	5.98 (6.06)	14.64 (14.14)
$[V_4]$	$C_{22}H_{26}O_2N_4S$	410	65.17 (64.39)	5.72 (6.34)	14.61 (13.65)
$[V_5]$	$C_{23}H_{28}O_2N_4S$	424	64.42 (65.09)	6.09 (6.60)	12.18 (13.09)
$[V_6]$	$C_{24}H_{30}O_2N_4S$	438	65.20 (65.75)	7.20 (6.84)	12.23 (12.78)
$[V_7]$	$C_{25}H_{32}O_2N_4S$	452	66.67 (66.37)	7.08 (7.07)	12.66 (12.38)
$[V_8]$	$C_{26}H_{34}O_2N_4S$	466	66.88 (66.95)	7.36 (7.29)	12.04 (12.01)
$[V_9]$	$C_{27}H_{36}O_2N_4S$	480	67.99 (67.50)	7.64 (7.50)	11.38 (11.66)
$[VI_2]$	$C_{30}H_{42}O_2N_4S$	522	69.34 (68.96)	8.34 (8.04)	11.41 (10.82)
$[VI_1]$	$C_{20}H_{20}O_3N_4S$	396	61.51 (60.60)	5.00 (5.05)	13.77 (14.14)
$[VI_2]$	$C_{21}H_{22}O_3N_4S$	410	60.65 (61.46)	5.71 (5.36)	14.02 (13.65)
$[VI_3]$	$C_{22}H_{24}O_3N_4S$	424	62.26 (62.36)	6.39 (5.66)	13.98 (13.20)
$[VI_5]$	$C_{24}H_{28}O_3N_4S$	452	62.95 (63.51)	6.88 (6.19)	13.15 (12.28)
$[VI_7]$	$C_{26}H_{32}O_3N_4S$	480	64.15 (65.000)	6.68 (6.66)	12.20 (11.66)

low molar mass mesogens. A graphical representation of the enthalpy changes for series $[V_n]$ compounds associated with $Cr \rightarrow N$, $N \rightarrow I$, $SmA \rightarrow N$, $Cr \rightarrow SmA$, and $Cr \rightarrow SmC$ phase transitions as a function of the number (n) of carbon atoms in the lateral alkoxy chain is given in Fig. 3. The odd-even effect for $N \rightarrow I$ and $SmA \rightarrow N$ transitions was observed. The enthalpy changes associated with crystallization decreased from 28.29 to 17.01 kJ/mol indicating effect of chain length on the crystallization behavior. Even though enthalpy

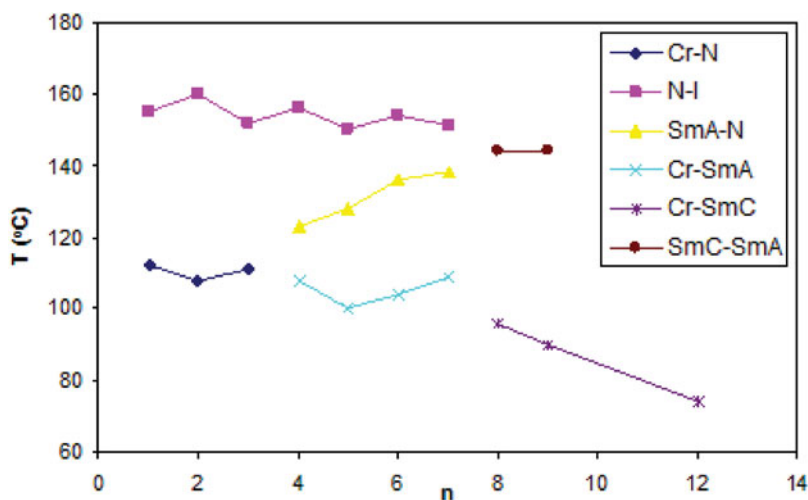
**Figure 1.** Dependence of transition temperatures on the increasing number of carbon atoms (n) in the terminal alkoxy chains for the $[V_n]$ series compounds.

Table 2. Phase transition temperatures and enthalpies data of series [V_n] compounds

Compound	Transition	Temperature °C	ΔH kJ mol ⁻¹	ΔS J K ⁻¹ mol ⁻¹
[V ₁]	Cr→Cr	80	—	—
	Cr→N	112	28.95	75.24
	N→I	155	0.59	1.40
[V ₂]	Cr→N	108	27.49	72.14
	N→I	160	0.65	1.54
[V ₃]	Cr→N	111	26.14	68.19
	N→I	152	0.97	2.30
[V ₄]	Cr→SmA	108	19.37	77.16
	SmA→N	123	4.36	43.54
	N→I	156	0.79	1.86
[V ₅]	Cr→SmA	100	17.01	45.65
	SmA→N	128	3.20	2.98
	N→I	150	1.19	2.81
[V ₆]	Cr→SmA	104	18.24	48.46
	SmA→N	136	3.28	5.67
	N→I	154	1.39	3.25
[V ₇]	Cr→SmA	109	21.73	56.95
	SmA→N	138	2.49	3.63
	N→I	151	0.99	2.35
[V ₈]	Cr→SmC	96	18.70	50.66
	SmC→SmA	144	2.07	4.97
	SmA→I	152	1.27	2.98
[V ₉]	Cr→SmC	90	17.03	46.92
	SmC→SmA	144	4.26	10.23
	SmA→I	148	—	—
[V ₁₂]	Cr→SmC	74	20.10	57.96
	SmC→I	146	7.74	18.45

Table 3. Phase transition temperatures and enthalpies data of series [VI_n] compounds

Compound	Transition	Temperature °C	ΔH kJ mol ⁻¹	ΔS J K ⁻¹ mol ⁻¹
[VI ₁]	Cr→N	119	24.60	62.77
	N→I	158	4.59	29.10
[VI ₂]	Cr→N	116	19.25	49.50
	N→I	168	0.29	0.66
[VI ₃]	Cr→N	112	17.41	45.22
	N→I	130	3.06	23.55
[VI ₅]	Cr→N	99	18.07	48.55
	N→I	121	0.59	1.50
[VI ₇]	Cr→SmA	103	16.48	43.84
	SmA→N	123	0.58	1.47
	N→I	112	0.78	1.84

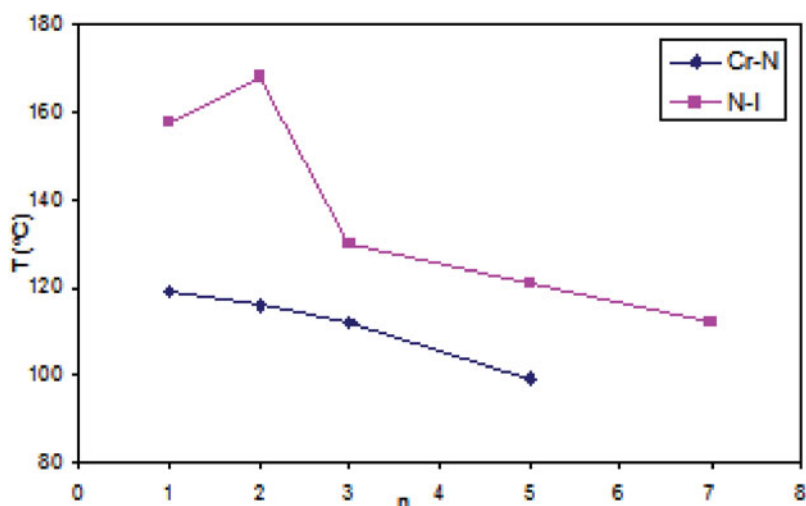


Figure 2. Dependence of transition temperatures on the increasing number of carbon atoms (n) in the terminal alkoxy chains for the $[VI_n]$ series compounds.

changes does not identify the mesophases, it can give an indication about existence different type of mesophases and further enthalpy changes associated with the crystalline phase are generally higher than that observed for mesophase as observed here.

All of the compounds in series $[V_n]$ show mesomorphic properties. The first three members of the series ($n = 1-3$) display an enantiotropic nematic (N) mesophase. The member with longest alkoxy chain ($n = 4-7$) exhibit an enantiotropic dimorphism smectic A (SmA) – N. For the members with $n = 8$ and 9 the nematic phase is not observed, those

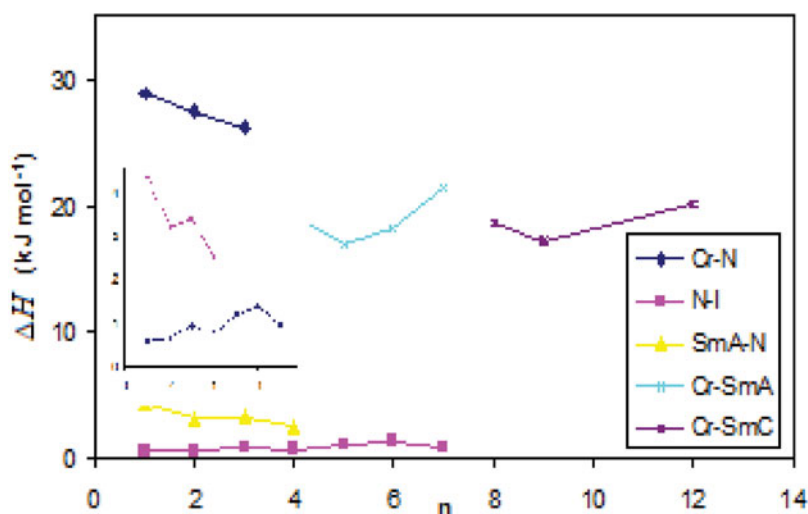


Figure 3. Dependence of enthalpy changes (ΔH) associated with transition temperatures on the increasing number of carbon atoms (n) in the terminal alkoxy chain for the $[V_n]$ series compounds.

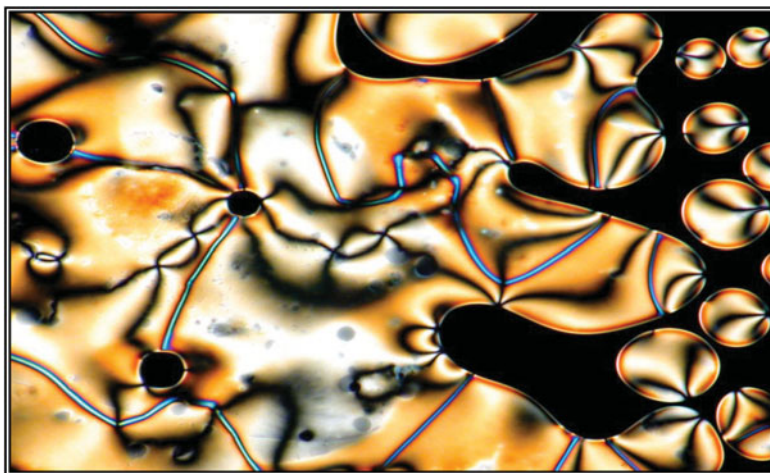


Figure 4. Mesophase texture of the N phase obtained on cooling. A schlieren texture and the typical nematic droplets ($200\times$ magnification) for the compound $[\mathbf{V}_3]$ at 137°C .

compounds show an enantiotropic dimorphism SmA and smectic C (SmC) mesophases, the member with $n = 12$ display only a SmC mesophase.

All the compounds of series $[\mathbf{VI}_n]$ also show mesomorphic properties. The compounds with $n = 1-3$ and 5 display an enantiotropic nematic. The last member ($n = 7$) exhibits exhibit an enantiotropic dimorphism nematic and SmA. These results illustrate the importance of the influence of terminal chain length on the occurrence of smectic order. It is likely that the lateral interaction giving rise to a layered smectic order is more favored for the compounds $n \geq 4$ (series $[\mathbf{V}_n]$) and compound $n = 7$ (series $[\mathbf{VI}_n]$), due to major volume occupied by the longer flexible alkoxy chain.



Figure 5. Mesophase texture of the SmA phase obtained on cooling. A typical focal-conic fan texture ($200\times$ magnification) for the compound $[\mathbf{VI}_7]$ at 120°C .

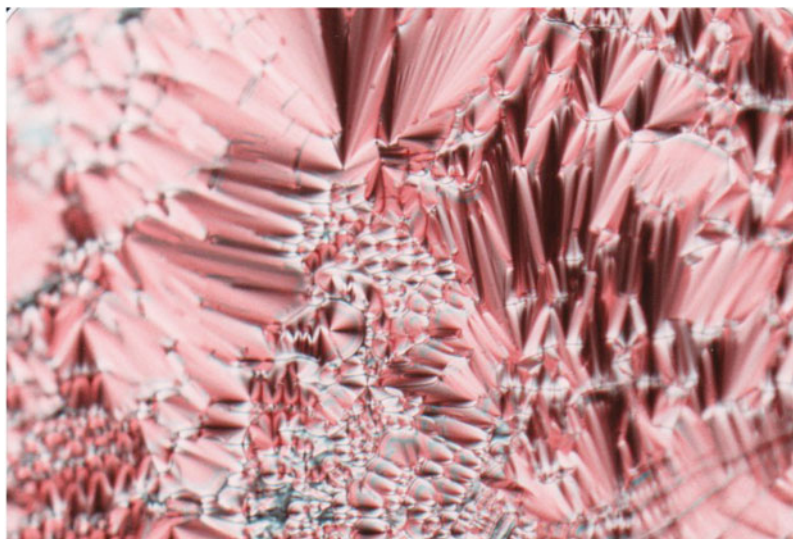


Figure 6. Mesophase texture of the SmC phase obtained on cooling. A broken focal-conic ($200\times$ magnification) for the compound $[V_{12}]$ at 135°C .

Compounds of series $[V_n]$ and $[VI_n]$ have the same central azo rigid core and the same 2-butylthio-1,3,4-oxadiazole moiety. The difference between those two series is in the lateral substituted chain. The results show that the alkoxy and carboxy alkyl chain has a profound influence on the mesomorphic properties. While compounds of series $[V_n]$ exhibit smectic mesophase starting with compound $n = 4$, compounds of series $[VI_n]$ display a smectic phase starting with compound $n = 7$. It seems likely that, in comparison, this is due to the carbonyl group which is coplanar with the aromatic rigid core; these compounds therefore have a major conjugated character and a major polarizability, making the lateral interaction in alkoxy chain more than that with carboxy alkyl chain which favors mesophase smectic phases formation [19].

The SmA, SmC, and N phases of the compounds of series $[V_n]$ and $[VI_n]$ were determined from textural observations by thermal microscopy under POM using heating and cooling cycles. Phase transition temperatures observed by POM were found to be in reasonable agreement with the corresponding DSC thermograms. The mesophases exhibited by $[V_n]$ and $[VI_n]$ compounds were identified from their optical textures, which were observed by POM, using the classification systems reported by Sackmann and Demus and Richter [20,21] and Gray and Goodby [22].

The nematic phase showed the typical schlieren texture with characteristic two- and four-brush singularities and the typical nematic droplets (Fig. 4). The SmA phase was characterized by the formation of a typical focal-conic fan texture (Fig. 5). Fig. 6 display the SmC mesophase texture which was identified by the appearance of a broken focal-conic texture.

References

- [1] Eich, M., & Wendorff, J. (1987). *Macromol. Chem. Rapid Commun.*, 8, 467.
- [2] Chapoy, L. L. (Ed.) (1985). *Advances in Liquid Crystalline Polymers*, Elsevier, London.
- [3] Parikh, V. B., & Menon, S. K. (2008). *Mol. Cryst. Liq. Cryst.*, 482, 71.

- [4] Pantalone, K., & Seed, A. J. (2002). *Liq. Cryst.*, 29, 945.
- [5] Parra, M., Vergara, J., Alderete, J., & Zuniga, C. (2004). *Liq. Cryst.*, 31, 1531.
- [6] Meyer, E., Joussef, A. C., Gallardo, H., & Bortoluzzi, A. J. (2003). *J. Mol. Struct.*, 655, 361.
- [7] Parra, M., Vergara, J., Soto, E., Sierra, T., & Serrano, J. L. (2004). *Liq. Cryst.*, 32, 457.
- [8] Han, J., Wang, J., Zhang, F., Zhu, L., Pang, M., & Meng, J. (2008). *Liq. Cryst.*, 35, 1205.
- [9] Parra, M., Hernandez, S., Alderete, J., & Zuniga, C. (2000). *Liq. Cryst.*, 27, 995.
- [10] Parra, M., Hidalgo, P., Carrasco, E., Barbera, J., & Silvino, L., (2006). *Liq. Cryst.*, 33, 875.
- [11] Cioanca, E. R., Epure, E. L., Carlescu, I., Lisa, G., Wilson, D., Hurduc, N., & Scutarui, A. (2011). *Mol. Cryst. Liq. Cryst.*, 537, 51.
- [12] Bai, B., Wang, H., Lin, X., Ran, X., Chengxiao Zhao, C., & Li, M. (2012). *Letters in Org. Chem.*, 76.
- [13] Tomma, J. H., Roui'l, I. H., & Al-Dujaili, A. H. (2009). *Mol. Cryst. Liq. Cryst.*, 501, 3.
- [14] Roui'l, I. H., Al-Mahdawi, M. T. S., Latif, I. A., Khilili, F. I., & Al-Dujaili A. H. (2011). *J. Chem. Chem. Eng.*, 5, 946.
- [15] Girdziunaite, D., Tschierske, C., Novotna, E., & Kresse, H. (1991). *Liq. Cryst.*, 10, 937.
- [16] Parra, M., Belmar, J., Zunza, H., Zuniga, C., Fuentes, G., & Martinez, R. (1995). *J. Prakt. Chem.*, 337, 239.
- [17] Kim, J. H. Park, J. H. & Lee, H. (2003). *Chem. Mater.*, 15, 3414.
- [18] Parra, M., Villouta, S. H., Vera, V., Belmar, J., Zuniga, C., & Zunza, H. (1997). *Z. Naturforsch.*, 52b, 1533.
- [19] Goodby, J. W. (1981). *Mol. Cryst. liq. Cryst.*, 75, 179.
- [20] Sackmann, H., & Demus, D. (1966). *Mol. Cryst. liq. Cryst.*, 2, 81.
- [21] Richter, D. (1980) "Textures of Liquid Crystals", VEB Deutscher Verlag fur Grundstoffindustrie, Leipzig.
- [22] Gray, G. W., & Goodby, J. W. (1984). "Smectic Liquid Crystals: Textures and Structures", Leonard Hill, London.